Mechanism underlying insulin uptake in alveolar epithelial cell line RLE-6TN

Keisuke Oda [a], Ryoko Yumoto [a], Junya Nagai [a], Hirokazu Katayama [b], Mikihisa Takano [a,*]

[a] *Department of Pharmaceutics and Therapeutics, Graduate School of Biomedical Sciences, Hiroshima University; 1-2-3 Kasumi, Minami-ku, Hiroshima 734-8553, Japan*
[b] *Faculty of Pharmacy and Pharmaceutical Sciences, Fukuyama University, Fukuyama, Japan*

*Corresponding author. Department of Pharmaceutics and Therapeutics, Graduate School of Biomedical Sciences, Hiroshima University; 1-2-3 Kasumi, Minami-ku, Hiroshima 734-8553, Japan.
Tel.: +81-82-257-5315; Fax: +81-82-257-5319.
E-Mail address: takanom@hiroshima-u.ac.jp (M. Takano).

Abstract

For the development of efficient pulmonary delivery systems for protein and peptide drugs, it is important to understand their transport mechanisms in alveolar epithelial cells. In this study, the uptake mechanism for FITC-insulin in cultured alveolar epithelial cell line RLE-6TN was elucidated. FITC-insulin uptake by RLE-6TN cells was time-dependent, temperature-sensitive, and concentration-dependent. The uptake was inhibited by metabolic inhibitors, cytochalasin D, clathrin-mediated endocytosis inhibitors, and dynasore, an inhibitor of dynamin GTPase. On the other hand, no inhibitory effect was observed with caveolae-mediated endocytosis inhibitors and a macropinocytosis inhibitor. Intracellular FITC-insulin was found to be partly transported to the basal side of the epithelial cell monolayers. In addition, colocalization of FITC-insulin and LysoTracker Red was observed on confocal laser scanning microscopy, indicating that FITC-insulin was partly targeted to lysosomes. In accordance with these findings, SDS-PAGE/fluoroimage analysis showed that intact FITC-insulin in the cells was eliminated with time. The possible receptor involved in FITC-insulin uptake by RLE-6TN cells was examined by using siRNA. Transfection of the cells with megalin or insulin receptor siRNA successfully reduced the corresponding mRNA expression. FITC-insulin uptake decreased on the transfection with insulin receptor siRNA, but not that with megalin siRNA. These results suggest that insulin is taken up through endocytosis in RLE-6TN cells, and after the endocytosis, the intracellular insulin is partly degraded in lysosomes and partly transported to the basal side. Insulin receptor, but not megalin, may be involved at least partly in insulin endocytosis in RLE-6TN cells.

Keywords: Alveolar epithelial cells; Insulin; Endocytosis; Dynamin; Megalin; Insulin receptor

1. Introduction

The lung is important as a possible administration route for drugs because of its large alveolar surface area and extremely thin epithelial barrier (Colthorpe et al., 1992). These structural features would be advantageous for the absorption of small, lipophilic drugs through a passive diffusion, but not to the absorption of protein and peptide drugs of large molecular sizes.

The alveolar region of the lung is lined with a continuous epithelium comprising type I and type II epithelial cells. Squamous type I cells cover 90 - 95% and cuboidal type II cells cover 5 - 10% of the alveolar surface area, though the number of type II cells is greater than that of type I cells (Kim and Malik, 2003). Using primary cultured alveolar epithelial cells, we previously reported that the uptake clearance of albumin was much greater in type II than in type I cells. Assuming that the number of type II cells is about 1.5-fold of that of type I cells, the contribution of type II cells to total albumin uptake was estimated to be more than 75% (Ikehata et al., 2008). Similarly, the contribution of type II cells to total insulin uptake was estimated to be more than 50% (Ikehata et al., 2009). Thus, though the surface area occupied by type II cells is quite small, type II cells may play an important role in the uptake of protein and peptide drugs in the lung.

The mechanisms for the clearance of various proteins and peptides from the alveolar space have been widely studied, and among the mechanisms proposed, endocytosis (transcytosis) is probably the most important (Hastings et al., 2004; Kim and Malik, 2003). Though a primary culture is a good experimental system, it is not suitable for an experiment involving a long-time treatment such as siRNA study, because type II cells in primary culture transdifferentiate into type I-like cells with time. Therefore, an established cell line would be an alternative and a useful experimental system for studying the alveolar transport of drugs. RLE-6TN cells have several characteristics similar to alveolar type II epithelial cells (Driscoll et al., 1995), and we have utilized RLE-6TN cells to clarify the transport mechanism for albumin (Yumoto et al., 2006).

Insulin is an important therapeutic drug for the treatment of diabetes mellitus. Recently, the lung has attracted a great deal of interest as an alternative administration route, and clinical research has confirmed the efficacy and safety of inhaled insulin in the treatment of diabetes mellitus (Agu et al., 2001; Galan et al., 2006; Scheuch et al., 2006). Unfortunately, inhaled insulin (Exbera®) has been withdrawn from the market, predominantly because of its low bioavailability and high cost (Siekmeier and Scheuch, 2008). However, information concerning insulin transport in alveolar epithelial cells is

still lacking, and understanding of its mechanisms may facilitate the development of more efficient form of inhaled insulin in the future. In this study, the mechanisms underlying insulin uptake and the fate of intracellular insulin were examined in RLE-6TN cells.

2. Materials and methods

2.1. Materials

Dulbecco's Modified Eagle's medium: Nutrient Mixture F-12 (Ham) (1:1) (DMEM/F-12), trypsin-EDTA, penicillin-streptomycin, Lipofectamine™ 2000, LysoTracker® Red DND-99 (LysoTracker Red) as a fluorescent lysosomal marker, and rat megalin siRNA were purchased from Invitrogen (Grand Island, NY, USA). Fetal bovine serum (FBS) was purchased from Biological Industries Ltd. (Kibbutz Beit Haemek, ISRAEL). Fluorescein isothiocyanate-labeled insulin from bovine pancreas (FITC-insulin), phenylarsine oxide (PAO), indomethacin (IND), nystatin (NYS), 5-(N-ethyl-N-isopropyl) amiloride (EIPA), and cytochalasin D (Cyto D) were purchased from Sigma-Aldrich (St. Louis, MO, USA). Chlorpromazine (CPZ) and 2,4-dinitrophenol (DNP) were purchased from Nacalai Tesque (Kyoto, Japan). 2-Deoxy-D-glucose (2DOG) was purchased from Kanto Chemical Co. (Tokyo, Japan) and sodium azide (NaN_3) from Katayama Chem. (Tokyo, Japan). Hoechst 33342 solution as a fluorescent nucleus marker, and HilyMax were purchased from Wako Pure Chemical Ind. (Osaka, Japan). ReverTra Ace and SYBR Green were from TOYOBO (Osaka, Japan). Rat insulin receptor siRNA was purchased from Santa Cruz Biotechnology (Santa Cruz, CA, USA). [^{3}H]Gentamicin sulfate (7.4 GBq/g) was obtained from American Radiolabeled Chemicals (St. Louis, MO, USA). All other chemicals used for the experiments were of the highest purity commercially available.

2.2. Cell culture

RLE-6TN cells were obtained from the American Type Culture Collection (ATCC no. CRL-2300; Manassas, VA, USA) and were cultured as described previously (Tagawa et al., 2008; Yumoto et al., 2006). The cells were used for the experiments on the seventh day after seeding between passages 48 and 65.

2.3. Uptake of FITC-insulin by RLE-6TN cells

Uptake experiments were performed as described previously (Ikehata et al., 2009; Tagawa et al., 2008; Takano et al., 2002). Briefly, RLE-6TN cells grown on 35-mm culture dishes were used. After removal of the culture medium, each dish was washed and preincubated with phosphate-buffered saline (137 mM NaCl, 3 mM KCl, 8 mM

Na_2HPO_4, 1.5 mM KH_2PO_4, 0.1 mM $CaCl_2$, and 0.5 mM $MgCl_2$, pH 7.4) (PBS buffer) supplemented with 5 mM D-glucose (PBS-G buffer) at 37°C for 10 min. Then, PBS-G buffer containing FITC-insulin (20 μg/ml) was added to each dish, and the cells were incubated at 37°C or 4°C for a specified period.

In the case of the concentration-dependence of insulin uptake, unlabeled insulin was dissolved in 0.1 M HCl, and then diluted with potassium free phosphate-buffered saline (137 mM NaCl, 8 mM Na_2HPO_4, 2 mM NaH_2PO_4, 0.1 mM $CaCl_2$, and 0.5 mM $MgCl_2$, pH 7.4) supplemented with 5 mM D-glucose (K^+ free PBS-G buffer). The pH of the solution was adjusted to 7.4 with 0.1 M NaOH. The kinetic parameters of insulin uptake were determined using the following Michaelis-Menten equation; $V = Vmax \cdot C^\gamma / (Km^\gamma + C^\gamma)$, where V is the uptake rate of insulin (μg/mg protein/60 min), C is the concentration of insulin, Vmax is the maximal uptake rate, Km is the apparent Michaelis constant, and γ is the Hill coefficient. The nonlinear curve was fitted with the KaleidaGraph program.

For inhibition studies, RLE-6TN cells were preincubated with PBS or PBS-G buffer at 37°C or 4°C with or without an inhibitor as follows; 1 mM DNP and 10 mM NaN_3 plus 5 mM 2DOG for 10 min in PBS buffer, 300 μM IND and 50 μM CPZ for 10 min in PBS-G buffer, 50 μM NYS, 5 μM PAO and 10 - 60 μM dynasore for 10 min, 40 μM Cyto D for 15 min, and 50 μM EIPA for 30 min in PBS-G buffer containing 0.5% DMSO. The same vehicle was used for each control experiment. Then, the cells were incubated with 1 ml of the buffer containing FITC-insulin with or without (control) an inhibitor at 37°C or 4°C for a specified period. PAO was only used in the preincubation buffer and was not added to the uptake buffer.

At the end of the incubation, the cells were rinsed three times with ice-cold PBS buffer or K^+-free PBS buffer (for the study of concentration-dependent insulin uptake) followed by scraping with a rubber policeman. Then, the cells were washed with PBS or K^+-free PBS buffer by centrifugation at 9838 g for 3 min at 4 °C twice, and the final pellet was solubilized in 0.1% Triton X-100 in PBS buffer without $CaCl_2$ and $MgCl_2$ for 30 min at room temperature, followed by centrifugation at 5600 g for 3 min. The supernatant was used for fluorescence and protein assays. The fluorescence of FITC-insulin was measured using a Hitachi fluorescence spectrophotometer F-3000 (TOKYO, Japan) at excitation and emission wavelengths of 500 and 520 nm, respectively. Protein contents were determined by the Lowry method with bovine serum albumin as the standard.

2.4. Transport of intracellular FITC-insulin to the basal side of the epithelial

monolayers

RLE-6TN cells were seeded at 80,000 cells/cm^2 on Transwell inserts (24 mm diameter inserts, 0.4 μm pore size, Corning Incorporated, NY, USA) and cultured for 10 days. To measure the transport of intracellular FITC-insulin to the basal side of the epithelial monolayers, cells grown on Transwell inserts were incubated with FITC-insulin (200 μg/mL) for 60 min. After washing, the cells were incubated with fresh PBS-G buffer without FITC-insulin at 37°C for a specified period. Remaining amount of FITC-insulin in the cells and transported amount of FITC-insulin from the cells to the basal side were measured using a fluorescence spectrophotometer.

2.5. Confocal laser scanning microscopy

RLE-6TN cells were grown on 35-mm glass-bottom culture dishes for 5 days. The cells were incubated with FITC-insulin (20 μg/ml), LysoTracker Red (75 nM), and Hoechst 33342 (10 μM) for 30 min at 37°C or 4°C, and after washing the cells with ice-cold PBS buffer three times for 5 min each, the fluorescence in the cells was visualized by confocal laser scanning microscopy (LSM5 Pascal, Carl ZEISS, Germany).

2.6. Pulse-chase analysis of intact FITC-insulin in RLE-6TN cells

To evaluate the intactness of FITC-insulin in RLE-6TN cells, the cells were incubated with FITC-insulin for 60 min at 37°C, and after washing, the cells were further incubated with PBS-G buffer without FITC-insulin for 30, 60, or 90 min at 37°C. The cell samples were solubilized in a loading buffer consisting of 2% SDS, 50 mM Tris-HCl, and 10% glycerol. Then, each sample was subjected to SDS-polyacrylamide gel electrophoresis (PAGE) on 15% polyacrylamide gels. After the SDS-PAGE, the fluorescence intensity of the gel was analyzed with a fluoroimage analyzer FLA-2000 (Fuji Photo Film, Tokyo, Japan).

2.7. Transfection with siRNAs, and uptake studies on FITC-insulin and [^{3}H]gentamicin

RLE-6TN cells were seeded at a density of 18 x 10^4 cells/well on 12-well plates or 8 x 10^4 cells/well on 24-well plates. After 24 hr, cells were transfected with a megalin-specific siRNA using HilyMax or an insulin receptor-specific siRNA using

Lipofectamine™ 2000, according to the manufacturer's instructions. The sequences of the megalin siRNAs were: sense, GCUAUUGUAUUAGAUCCUUtt and anti-sense, AAGGAUCUAAUACAAUAGCtt. Non-targeting siRNA was used as a control in an identical manner. Briefly, cells were transfected with siRNA (100 nM) complexed with HilyMax (6 μl/ml) or Lipofectamine™ 2000 (2 μl/ml) for 24 hr. After 48 hr, the efficiency of siRNA silencing was evaluated by Western blot and real-time PCR analyses, and uptake study was performed as described in section 2.3. In the case of [^{3}H]gentamicin, the cells were solubilized in 0.1 M NaOH, and then the amount of substrate taken up by the cells was measured by counting the radioactivity. Protein contents were determined by the Bradford method.

2.8. RT-PCR analysis of insulin receptor mRNA expression in RLE-6TN cells and primary cultured rat alveolar type II epithelial cells

Rat alveolar type II epithelial (AT II) cells were isolated from Sprague-Dawley male rats as described previously (Ikehata et al., 2008, 2009). Total RNA was extracted from RLE-6TN cells and AT II cells using an RNeasy Mini kit (Qiagen, Valencia, CA, USA), and RT-PCR was performed as described previously (Takano et al., 2009). The primers were: sense, 5'- ATGGGACCACTGTACGCTTC -3' and antisense, 5'-CATTGAGGAACTCGATCCGT -3' for insulin receptor (expected size of PCR product, 275 bp). The PCR products were separated by electrophoresis on 2.0% agarose gels.

2.9. Real-time PCR analysis

Total RNA (0.8 μg), in a final volume of 20 μl, was reverse transcribed into cDNA using ReverTra Ace. Real-time PCR was performed on a BioFlux LineGene system (TOYOBO, Osaka, Japan) using SYBR Green. The PCR conditions were: initial denaturation in one cycle of 1 min at 95°C, followed by 40 cycles of 5 sec at 95°C (denaturation), 5 sec at 60°C (annealing), and 15 sec at 72°C (extension). The primers were: sense, 5'-AAAGTGGCCCTGGCAGTTC-3' and antisense, 5'-GAAGGATCTATGGGCCTTCCA-3' for megalin; sense, 5'-CGTCATTCACAACAACAAGTG-3' and antisense, 5'-ATGGTCTTCTCGCCTTCG-3' for insulin receptor; and sense, 5'-AGCCCAGAACATCATCCCTG-3' and antisense, 5'-CACCACCTTCTTGATGTCATC-3' for GAPDH. The expression level of each mRNA was normalized as to that of GAPDH, a house-keeping gene.

2.10. Western blot analysis

The amount of megalin in RLE-6TN cells was determined by Western blot analysis as described previously (Nagai et al., 2001). Proteins were extracted from the cells using cell lysis buffer comprising 150 mM NaCl, 5mM EDTA, 1mM PMSF, 10 mM Tris, 1% Triton-X100, 0.1% SDS, and 1% sodium deoxycholate (pH 7.4). The lysates were centrifuged at 8,720 g for 5 min at 4°C and the supernatants were stored at - 80°C. 8 μg protein extracts were subjected to SDS-PAGE on 6% polyacrylamide gels, and then transferred to polyvinylidene difuluoride (PVDF) membranes. After blotting, the membranes were blocked with 0.5% skim milk and subsequently incubated with anti-rat megalin rabbit anti-serum (1:1000 dilution). The membranes were washed three times in TBS-T (20.5 mM Tris, 150 mM NaCl, 0.05% Tween20, pH 7.5), and then incubated with horseradish peroxidase-conjugated anti rabbit IgG antibodies (1:2000 dilution). After washing three times in TBS-T, the antibody complexes were visualized with Amersham ECL Plus Detection reagents. The blocking and antibody incubation processes were performed by use of an SNAP i.d. system (Millipore, Billerica, MA, USA). The optical densities of immunoreactive proteins were determined with a computer-aided densitometer with NIH Image (the public domain program developed at the U.S. National Institutes of Health, Bethesda, MD, USA).

2.11. Statistical analysis

All data were expressed as means ± standard error of the mean (S.E.M.). Statistical analysis was performed by the Student‘s *t*-test or one-way ANOVA, followed by the Tukey-Kramer’s test for multiple comparisons. The level of significance was set at *$P<0.05$ or ** $P<0.01$.

3. Results

3.1. General characteristics of FITC-insulin uptake by RLE-6TN cells

In order to understand the general characteristics of FITC-insulin uptake by RLE-6TN cells, the time- and temperature-dependence of FITC-insulin uptake were measured (Fig. 1A). FITC-insulin was taken up by the cells at 37°C, and the uptake increased with time for up to 60 min. The apparent uptake at 4°C, probably reflecting cell surface binding, was also time-dependent, but was significantly lower than that at 37°C. Next, the uptake of insulin in 60 min was measured in the concentration range of 20-2000 μg/ml at 37°C. As shown in Fig. 1B, insulin uptake by RLE-6TN cells showed a sigmoid curve (Hill coefficient, 1.2) and saturation kinetics. The apparent Michaelis constant (K_m) and maximum uptake rate (V_{max}) were calculated to be 1892 μg/ml and 208.3 μg/mg protein/60 min, respectively. In the following uptake experiments, the amount of FITC-insulin taken up into the cells (specific uptake) was determined by subtracting the cell surface binding at 4°C from the total cell association at 37°C.

3.2. Endocytic pathway for FITC-insulin

The effects of metabolic inhibitors on FITC-insulin uptake by RLE-6TN cells were examined. Treatment of the cells with NaN_3 plus 2DOG or DNP significantly inhibited FITC-insulin uptake (Fig. 2A). We then examined the effects of various endocytosis inhibitors on FITC-insulin uptake. Cyto D, an F-actin polymerization inhibitor, inhibited the FITC-insulin uptake. PAO and CPZ, clathrin-mediated endocytosis inhibitors, also inhibited FITC-insulin uptake, though the extents of inhibition were fairly low. On the other hand, no inhibitory effect was observed on treatment with NYS and IND, caveolae-mediated endocytosis inhibitors, or on the treatment with EIPA, a macropinocytosis inhibitor. Furthermore, the effect of dynasore, a dynamin GTPase inhibitor, on FITC-insulin uptake by RLE-6TN cells was examined (Fig. 2B). FITC-insulin uptake was inhibited by dynasore in a concentration-dependent manner.

3.3. Transport of intracellular FITC-insulin to the basal side of the epithelial monolayers

In order to characterize the transport of intracellular FITC-insulin to the basal side of epithelial monolayers, RLE-6TN cells grown in a Transwell chamber were used. We

first attempted to quantitate the transcellular transport of FITC-insulin, but RLE-6TN cell monolayers in the Transwell chamber were so leaky that FITC-insulin was predominantly transported from the apical side to the basal side via a paracellular route. In fact, the TEER values obtained for these monolayers were much lower than those reported for the alveolar epithelium in the lung, being around 100 - 170 $\Omega \cdot cm^2$ even at 10 days after seeding. Under these conditions, the paracellular transport was too high to quantitate transcellular transport (transcytosis) properly. Therefore, in order to quantitate transcytosis of FITC-insulin, the efflux of FITC-insulin preloaded into the cells to the basal side was measured. Intracellular FITC-insulin was gradually transported to the basal side (Fig. 3A). As shown in Fig. 3B, SDS-PAGE/fluoroimage analysis revealed that most of the FITC-insulin transported to the basal side was intact. In accordance with the efflux of FITC-insulin, the amount of FITC-insulin remaining in the cells decreased after 2.5 hr incubation with PBS-G buffer (Fig. 3C).

3.4. Intracellular localization of FITC-insulin taken up by RLE-6TN cells

Intracellular localization of FITC-insulin was examined by confocal laser scanning microscopy. When RLE-6TN cells were incubated with FITC-insulin at 37^{o}C, punctate localization of fluorescence was observed in the cells (Fig. 4A). On the other hand, when the cells were incubated with FITC-insulin at 4^{o}C, intracellular localization of FITC-insulin was not observed (Fig. 4D). Figure 4B shows the fluorescence of LysoTracker Red, a lysosomal marker, simultaneously added to the uptake buffer with FITC-insulin at 37^{o}C. As shown in Figure 4C, colocalization of FITC-insulin and LysoTracker Red was observed at 37^{o}C, indicating that part of the FITC-insulin taken up by the cells was targeted to lysosomes.

3.5. Degradation and elimination of intracellular FITC-insulin after being taken up by RLE-6TN cells

The intactness of FITC-insulin in cells was evaluated with a fluoroimage analyzer after SDS-PAGE (Fig. 5A). Figure 5B shows the results of pulse-chase analysis, the FITC-insulin taken up by RLE-6TN cells being gradually degraded/eliminated over time. Using semilogarithmic plots (Fig. 5C), the half-life of FITC-insulin in the cells was calculated to be 77 min.

3.6. siRNA transfection study

Megalin is a candidate receptor for insulin (Orlando et al., 1998). Therefore, we first attempted to clarify the role of megalin in FITC-insulin uptake by RLE-6TN cells by transfection with megalin siRNA. Transfection of cells with megalin-specific siRNA reduced the mRNA expression level (Fig. 6A) and the protein expression level (Fig. 6B) of megalin. Using these megalin knockdown cells, the uptake of [^{3}H]gentamicin, which is well known to be a megalin ligand (Moestrup et al., 1995), and FITC-insulin were examined. As shown in Fig. 7A, the uptake of [^{3}H]gentamicin was significantly reduced in RLE-6TN cells transfected with megalin-specific siRNA compared with those transfected with nonspecific (control) siRNA. In contrast, FITC-insulin uptake was not affected by transfection with megalin siRNA (Fig. 7B).

Next, we examined the role of insulin receptor in FITC-insulin uptake by using insulin receptor siRNA. The mRNA expression of insulin receptor was confirmed by RT-PCR in RLE-6TN cells as well as in primary cultured type II epithelial cells (Fig. 8A). Transfection of RLE-6TN cells with the siRNA significantly reduced the mRNA expression of insulin receptor. The uptake of FITC-insulin was significantly reduced in the RLE-6TN cells transfected with insulin receptor siRNA compared with those transfected with control siRNA.

4. Discussion

We first examined the general characteristics of FITC-insulin uptake by rat alveolar type II epithelial cell line, RLE-6TN. The uptake of FITC-insulin was time- and temperature-dependent (Fig. 1A), and showed saturation kinetics (Fig. 1B). Metabolic inhibitors potently inhibited the FITC-insulin specific uptake (temperature-sensitive uptake). In addition, an inhibitory effect of Cyto D, which is known to inhibit F-actin polymerization and therefore inhibit various endocytic processes, on FITC-insulin uptake was observed (Fig. 2). These results indicate that energy-dependent, saturable mechanism, most likely receptor-mediated endocytosis, is involved in FITC-insulin uptake by RLE-6TN cells. These characteristics are essentially the same as those observed for primary cultured alveolar type II epithelial cells (Ikehata et al., 2009), though the apparent affinity seems to be somewhat lower in RLE-6TN cells.

There are numerous ways that endocytic cargo molecules are internalized from the surface of eukaryotic cells (Mayor and Pagono, 2007). Endocytic pathways are divided into at least four mechanisms; clathrin-mediated endocytosis, caveolae-mediated endocytosis, macropinocytosis and other types of endocytosis (clathrin- and caveolae-independent endocytosis). Clathrin-mediated endocytosis, which is the best characterized endocytosis pathway, involves many proteins such as clathrin and assembly protein (AP) 2. Caveolae-mediated endocytosis occurs through flask-shaped invaginations of the plasma membrane, and the involvement of intracellular protein caveolin-1 is known. In addition, dynamin, which is a large GTPase and functions in membrane tubulation and fission of budding vesiculo-tubular structures, is necessary for both clathrin- and caveolae-mediated endocytosis. Macropinocytosis accompanies the membrane ruffling that is induced in many types of cells upon stimulation by growth factors or other signals. Macropinocytosis generates relatively large vesicles (1 - 5 μm) that are associated with the formation of actin-dependent membrane ruffles. In alveolar epithelial cells, the endocytic pathway for insulin is unclear. Therefore, we further investigated the uptake mechanism for FITC-insulin focusing on three types of endocytosis; clathrin-mediated endocytosis, caveolae-mediated endocytosis and macropinocytosis.

PAO inhibits clathrin-mediated endocytosis by reacting with vicinal sulfhydryls to form stable ring structures (Visser et al., 2004). CPZ inhibits the process by inducing the loss of coated pits from the cell surface, probably by interacting with AP2 binding to membranes (Wang et al., 1993). In this study, both compounds slightly inhibited FITC-insulin uptake by RLE-6TN cells. We previously showed that FITC-albumin

uptake was inhibited by PAO and CPZ, and suggested the involvement of clathrin-mediated endocytosis in RLE-6TN cells (Yumoto et al., 2006). However, the extents of inhibition by these inhibitors were quite different between FITC-albumin and FITC-insulin uptake by RLE-6TN cells. FITC-albumin uptake was much more potently inhibited by PAO and CPZ (by 60 - 70%) than FITC-insulin uptake (by 18 - 20%). In addition, we recently reported that in primary cultured rat alveolar type II epithelial cells, the inhibition of FITC-insulin uptake by PAO and CPZ was not high (by 7 - 13%), and was statistically insignificant (Ikehata et al., 2009). Thus, clathrin-mediated endocytosis may be involved in FITC-insulin uptake by RLE-6TN cells, but its contribution may not be so high in alveolar type II epithelial cells. Another endocytosis inhibitor, dynasore, inhibited FITC-insulin uptake by RLE-6TN cells. The sensitivity of FITC-insulin uptake to dynasore in RLE-6TN cells was similar to that observed in primary cultured type II cells (Ikehata et al., 2009).

NYS and IND were used as inhibitors of caveolae-mediated endocytosis. NYS inhibits caveolae-mediated endocytosis by interacting with cholesterol in the plasma membrane (Sieczkarski and Whittaker, 2002), and IND inhibits the process by inhibiting the internalization of caveolae and the return of plasmalemmal vesicles to the cell surface (Smart et al., 1995). In fact, on confocal laser scanning microscopic analysis, we previously observed that the uptake of cholera toxin subunit B, which is a marker of caveolae-mediated endocytosis, was potently blocked by NYS and IND in RLE-6TN cells (Takano and Yumoto, 2011), indicating that the caveolae-mediated endocytosis pathway was functioning in RLE-6TN cells. However, the FITC-insulin uptake by RLE-6TN cells was not affected by these inhibitors (Fig. 2). Xu et al. (1996) reported that insulin enhanced macropinocytosis through insulin receptor activation in Chinese hamster ovary cells transfected with human insulin receptor. However, in this study, no inhibitory effect on FITC-insulin uptake was observed on treatment with EIPA, which inhibits Na^+/H^+ exchanger in the plasma membrane and inhibits macropinocytosis (Fig. 2). Therefore, neither caveolae-mediated endocytosis nor macropinocytosis would be involved in FITC-insulin uptake by RLE-6TN cells. The insensitivity of FITC-insulin uptake to the inhibitors of caveolae-mediated endocytosis in RLE-6TN cells was also similar to that observed in primary cultured type II cells (Ikehata et al., 2009). Additional pathways, which are energy-dependent but clathrin-, caveolae-, and macropinocytosis-independent, may be involved in FITC-insulin uptake by RLE-6TN cells.

As described above, FITC-insulin uptake by RLE-6TN cells was inhibited by dynasore, an inhibitor of a large GTPase dynamin. According to the classification of

endocytic pathways by Mayor and Pagano (2007), several endocytic pathways that are not associated with clathrin and caveolae are emerging. One of such pathways is dynamin-dependent, RhoA-regulated pathway. RhoA is a small GTPase, and has been found to regulate the internalization of β-chain of the interleukin-2 receptor; thus it is also called IL2Rβ pathway (Doherty and McMahon, 2009; Lamaze et al., 2001). Based on the above classification and the present results, FITC-insulin uptake may partly be mediated by clathrin- and caveolae-independent, but dynamin-dependent, RhoA-regulated pathway in RLE-6TN cells as well as in primary cultured alveolar type II epithelial cells.

In order to study the fate of FITC-insulin taken up by RLE-6TN cells, transport of FITC-insulin from the cells to the basal side of epithelial monolayers was examined using a Transwell chamber (Fig. 3). Intracellular FITC-insulin was gradually transported to the basal side mostly as an intact form. Some reports have suggested that inhaled insulin is transported across the alveolar epithelial barrier through passive diffusion (Bur et al., 2006). In contrast, our results may indicate that inhaled insulin is absorbed from the lung, at least in part, through transcytosis. Next, intracellular localization of FITC-insulin in RLE-6TN cells was evaluated by confocal laser scanning microscopy (Fig. 4). At 37^{o}C, punctate localization of FITC-insulin fluorescence was observed in the cells, supporting endocytic uptake of FITC-insulin. On the other hand, no fluorescence of FITC-insulin was observed at 4^{o}C. Thus, the apparent uptake observed at 4°C in Fig. 1 would reflect cell surface binding of FITC-insulin, as described above. In addition, it was suggested that part of the FITC-insulin taken up by the cells was targeted to lysosomes, as evidenced by the colocalization of FITC-insulin and LysoTracker Red. In accordance with these results, pulse-chase analysis with an SDS-PAGE/fluoroimage analyzer showed that intracellular FITC-insulin was gradually degraded and/or eliminated over time, probably due to the degradation in lysosomes and efflux from the cells.

The receptor involved in insulin endocytosis by alveolar epithelial cells is not clear at present. Recently, several possible receptors for insulin endocytosis in various types of cells have been reported, including megalin and insulin receptor (Guglielmo et al., 1998; Orlando et al., 1998). Megalin is a large glycoprotein (approximately 600 kDa) that functions as an endocytic receptor for multiple ligands including lysozyme, cytochrome c, albumin, and aminoglycosides (Christensen and Birn, 2001). The receptor belongs to the LDL receptor family, and is highly expressed in renal proximal tubule epithelial cells as well as in alveolar type II epithelial cells (Christensen and Birn, 2001; Kolleck et al., 2002). Using chemical cross-linking and cytochemical procedures,

Orlando et al. (1998) obtained potent evidence suggesting that megalin is an endocytic receptor for insulin in renal proximal tubules. Therefore, we first investigated the role of megalin in insulin endocytosis in RLE-6TN cells. The expression of megalin mRNA and protein in RLE-6TN cells was confirmed by real-time PCR and Western blot analysis, respectively (Fig. 6). Transfection of RLE-6TN cells with megalin-specific siRNA reduced the mRNA and protein expression levels of megalin, and [^{3}H]gentamicin uptake by the cells. Aminoglycoside antibiotics such as gentamicin are well known ligands of megalin, and the predominant role of megalin in the endocytosis of aminoglycosides in renal proximal tubular cells has been reported (Nagai et al., 2001; Schmitz et al., 2002; Watanabe et al., 2004). Thus, megalin-mediated endocytosis would occur in RLE-6TN cells. However, FITC-insulin uptake was not affected by transfection with megalin siRNA, indicating that megalin is not involved in insulin endocytosis in RLE-6TN cells.

Insulin receptor is suggested to be responsible for the uptake of insulin into certain types of cells (Guglielmo et al., 1998). We also verified the expression of insulin receptor mRNA in RLE-6TN cells as well as in primary cultured type II cells by RT-PCR analysis (Fig. 8A). Though one report suggested that insulin receptor appeared to be localized at the basal side of alveolar epithelial cells (Yamahara et al., 1994), the localization of insulin receptor in alveolar epithelial cells remains unclear. Therefore, we next examined the role of insulin receptor by using insulin receptor siRNA. Transfection of RLE-6TN cells with insulin receptor-specific siRNA successfully reduced its mRNA expression level and FITC-insulin uptake. Therefore, insulin receptor may be involved at least partly in insulin endocytosis in RLE-6TN cells. The involvement of other receptors such as insulin-like growth factor I receptor (IGF-IR), which is known to interact with insulin (Chisalita and Arnqvist, 2004), and scavenger receptors like SR-AI/II, which can bind to a variety of anionic proteins (Steinbrecher, 1999), needs to be examined in future.

In conclusion, FITC-insulin is taken up through endocytosis in alveolar epithelial cell line RLE-6TN, and after endocytosis, the intracellular FITC-insulin is partly degraded in lysosomes and partly transported to the basal side. Insulin receptor, but not megalin, may partly be involved in insulin endocytosis in RLE-6TN cells. These results constitute useful information for understanding the uptake mechanism and intracellular fate of insulin in alveolar epithelial cells.

Acknowledgements

We thank the Institute of Laboratory Animal Science, the Natural Science Center for Basic Research and Development, and the Analysis Center of Life Science, Hiroshima University for the use of their facilities. This work was supported in part by a Grant-in-Aid for Scientific Research from the Ministry of Education, Science, Sports, and Culture in Japan.

References

Agu, R.U., Ugwoke, M.I., Armand, M., Kinget, R., Verbeke, N., 2001. The lung as a route for systemic delivery of therapeutic proteins and peptides. Respir. Res. 2, 198-209.

Bur, M., Huwer, H., Lehr, C.M., Hagen, N., Guldbrandt, M., Kim, K.J., Ehrhardt, C., 2006. Assessment of transport of proteins and peptides across primary human alveolar epithelial cell monolayers. Eur. J. Pharm. Sci. 28, 196-203.

Chisalita, S.I., Arnqvist, H.J., 2004. Insulin-like growth factor I receptors are more abundant than insulin receptors in human micro- and macrovascular endothelial cells. Am. J. Physiol. Endocrinol. Metab. 286, E896-E901.

Christensen, E.I., Birn, H., 2001. Megalin and cubilin: synergistic endocytic receptors in renal proximal tubule. A. J. Physiol. Renal Physiol. 280, F562-573.

Colthorpe, P., Farr, S.J., Taylor, G., Smith, I.J., Wyatt, D., 1992. The pharmacokinetics of pulmonary-delivered insulin: a comparison of intratracheal and aerosol administration to the rabbit. Pharm. Res. 9, 764-768.

Doherty, G.J. and McMahon, H.T., 2009. Mechanisms of endocytosis. Annu. Rev. Biochem. 78, 857–902.

Driscoll, K.E., Carter, J.M., Iype, P.T., Kumari, H.L., Crosby, L.L., Aardema, M.J., Isfort, R.J., Cody, D., Chestnut, M.H., Burns, J.L., Leboeuf, R.A., 1995. Establishment of immortalized alveolar type II epithelial cell lines from adult rats. In Vitro Cell Dev. Biol. Anim. 7, 516-527.

Galan, B.E., Simsek, S., Tack, C.J., Heine, R.J., 2006. Efficacy and safety of inhaled insulin in the treatment of diabetes mellitus. Neth. J. Med. 64, 319-325.

Guglielmo, G.M.D., Drake, P.G., Baass, P.C., Authier, F., Posner, B.I., Bergeron, J.J., 1998. Insulin receptor internalization and signaling. Mol. Cell. Biochem. 182, 59-63.

Hastings, R.H., Folkesson, H.G., Matthay, M.A., 2004. Mechanisms of alveolar protein

clearance in the intact lung. Am. J. Physiol. Lung Cell Mol. Physiol. 286, 679–689.

Ikehata, M., Yumoto, R., Kato, Y., Nagai, J., Takano, M., 2009. Mechanism of insulin uptake in rat alveolar type II and type I-like epitherial cells. Biol. Pharm. Bull. 32, 1765-1769.

Ikehata, M., Yumoto, R., Nakamura, K., Nagai, J., Takano, M., 2008. Comparison of albumin uptake in rat type II and type I-like epithelial cells in primary culture. Pharm. Res. 25, 913-922.

Kim, K.J., Malik, A.B., 2003. Protein transport across the lung epithelial barrier. Am. J. Physiol. Lung Cell Mol. Physiol. 284, 247-259.

Kolleck, I., Wissel, H., Guthmann, F., Schlame, M., Sinha, P., Rustow, B., 2002. HDL-holoparticle uptake by alveolar type II cells: effect of vitamin E status. Am. J. Respir. Cell Mol. Biol. 27, 57-63.

Lamaze, C., Dujeancourt, A., Baba, T., Lo, C.G., Benmerah, A., Dautry-Varsat, A., 2001. Interleukin 2 receptors and detergent-resistant membrane domains define a clathrin-independent endocytic pathway. Mol. Cell 7, 661–671.

Mayor, S., Pagono, R.E., 2007. Pathways of clathrin-independent endocytosis. Nature Rev. Mol. Cell Bio. 8, 603-612.

Moestrup, S.K., Cui, S., Vorum, H., Bregengård, C., Bjørn, S.E., Norris, K., Gliemann, J., Christensen, E.I., 1995. Evidence that epithelial glycoprotein 330/megalin mediates uptake of polybasic drugs. J. Clin. Invest. 96, 1404-1413.

Nagai, J., Tanaka, H., Nakanishi, N., Murakami, T., Takano, M., 2001. Role of megalin in the renal handling of aminoglycosides. Am. J. Physiol. Renal Physiol. 281, F337-344.

Orlando, R.A., Rader, K., Authier, F., Yamazaki, H., Posner, B.I., Bergeron, J.J.M., Farquhar, M.G., 1998. Megalin is an endocytic receptor for insulin. J. Am. Soc. Nephrol. 9, 1759-1766.

Scheuch, G., Kohlhaeufl, M.J., Brand, P., Siekmeier, R., 2006. Clinical perspectives on

pulmonary systemic and macromolecular delivery. Adv. Drug Deliv. Rev. 58, 996-1008.

Schmitz, C., Hilpert, J., Jacobsen, C., Boensch, C., Christensen, E.I., Luft, F.C., Willnow, T.E., 2002. Megalin deficiency offers protection from renal aminoglycoside accumulation. J. Biol. Chem. 277, 618-622.

Sieczkarski, S.B., Whittaker, G.R., 2002. Dissecting virus entry via endocytosis. J. Gen. Virol. 83, 1535-1545.

Siekmeier, R., Scheuch, G., 2008. Inhaled insulin--does it become reality? J. Physiol. Pharmacol. 6, 81-113.

Smart, E.J., Estes, K., Anderson, R.G., 1995. Inhibitors that block both the internalization of caveolae and the return of plasmalemmal vesicles. Cold Spring Harb. Symp. Quant. Biol. 60, 243–248.

Steinbrecher, U.P., 1999. Receptors for oxidized low density lipoprotein. Biochim. Biophys. Acta 1436, 279-298.

Tagawa, M., Yumoto, R., Oda, K., Nagai, J., Takano, M., 2008. Low-affinity transport of FITC-albumin in alveolar type II epithelial cell line RLE-6TN. Drug Metab. Pharmacokinet. 23, 318-327.

Takano, M., Nishikawa, N., Kitahara, Y., Sasaki, Y., Murakami, T., Nagai, J., 2002. Cisplatin-induced inhibition of receptor-mediated endocytosis of protein in the kidney. Kidney Int. 62, 1707-1717.

Takano, M., Otani, Y., Tanda, M., Kawami, M., Nagai, J., Yumoto, R., 2009. Paclitaxel-resistance conferred by altered expression of efflux and influx transporters for paclitaxel in the human hepatoma cell line, HepG2, Drug Metab. Pharmacokinet. 24, 418-427.

Takano, M., Yumoto, R., 2011. Transport of proteins and peptides and its regulation in alveolar epithelial cells. Membrane. 36, 145-153.

Visser, C.C., Stevanovic, S., Voorwinden, L.H., Gaillard, P.J., Crommelin, D.J., Danhof, M., De Boer, A.G., 2004. Validation of the transferrin receptor for drug targeting to brain capillary endothelial cells in vitro. J. Drug Target. 12, 145-150.

Wang, L.H., Rothberg, K.G., Anderson, R.G., 1993. Mis-assembly of clathrin lattices on endosomes reveals a regulatory switch for coated pit formation. J. Cell Biol. 123, 1107-1117.

Watanabe, A., Nagai, J., Adachi, Y., Kitahara, Y., Murakami, T., Takano, M., 2004. Targeted prevention of renal accumulation and toxicity of gentamicin by aminoglycoside binding receptor antagonists. J. Control. Release 95, 423-433.

Xu, G., Howland, J., Rothenberg, P.L., 1996. Insulin and secretagogues differentially regulate fluid-phase pinocytosis in insulin-secreting ß-cells. Biochem. J. 318, 623-629.

Yamahara, H., Lehr, C.M., Lee, V.H.L., Kim, K.J., 1994. Fate of insulin during transit across rat alveolar epithelial cell monolayers. Eur. J. Pharm. Biopharm. 40, 294-298.

Yumoto, R., Nishikawa, H., Okamoto, M., Katayama, H., Nagai, J., Takano, M., 2006. Clathrin-mediated endocytosis of FITC-albumin in alveolar type II epithelial cell line RLE-6TN. Am. J. Physiol. Lung Cell Mol. Physiol. 290, L946-955.

Figure legends

Fig. 1. General characteristics of FITC-insulin uptake by RLE-6TN cells. (A) Time- and temperature-dependence of FITC-insulin uptake by RLE-6TN cells. The uptake of FITC-insulin (20 μg/ml) by confluent monolayers of RLE-6TN cells was measured at 37°C (●) or 4°C (○). Specific uptake (▲) was estimated by subtracting the cell surface binding at 4°C from the total cell association at 37°C. (B) Concentration-dependence of insulin uptake by RLE-6TN cells. The uptake of FITC-insulin (20 μg/ml) in the presence of various concentrations of unlabeled insulin for 60 min was measured at 37°C. The apparent Michaelis constant (Km), maximum uptake rate (Vmax), and Hill coefficient were calculated to be 1892 μg/ml, 208.3 μg/mg protein/60 min, and 1.2, respectively, by using the Michaelis-Menten equation. Each point represents the mean ± S.E.M. of three monolayers.

Fig. 2. Effects of various inhibitors on FITC-insulin uptake by RLE-6TN cells. (A) Cells were treated with various inhibitors as described under Materials and Methods. The uptake of FITC-insulin (20 μg/ml) with or without (control) an inhibitor for 60 min was measured at 37°C or 4°C. The dotted line indicates the control level. (B) Effects of various concentrations of dynasore on FITC-insulin (20 μg/ml) uptake. Specific uptake was estimated by subtracting the cell surface binding at 4°C from the total cell association at 37°C. Each point represents the mean ± S.E.M. of three monolayers. **P<0.01, significantly different from each control.

Fig. 3. Transport of intracellular FITC-insulin to the basal side of RLE-6TN monolayers. (A) Cells preloaded with FITC-insulin for 60 min were incubated with PBS-G buffer in the absence of FITC-insulin for a specified period. The amount of FITC-insulin transported to the basal side was measured. (B) The intactness of transported FITC-insulin was evaluated with a fluoroimage analyzer after separation by SDS-PAGE. (C) The amount of FITC-insulin remaining in the cells was measured after incubation with PBS-G buffer for 2.5 hr. Each point represents the mean ± S.E.M. of three monolayers. **P<0.01, significantly different from that at 0 hr.

Fig. 4. Intracellular localization of FITC-insulin**.** RLE-6TN cells were observed by confocal laser scanning microscopy after incubation with FITC-insulin (20 μg/ml), LysoTracker Red (75 nM), and Hoechst 33342 (10 μM) for 30 min at 37°C (A, B, C) or 4°C (D). (A, D) FITC-insulin (green), (B) LysoTracker Red (red), and Hoechst 33342 (blue). Colocalization of fluorescence derived from FITC-insulin and LysoTracker Red

is shown by a yellow color in C (merged).

Fig. 5. Estimation of intact FITC-insulin in RLE-6TN cells. Cells preloaded with FITC-insulin for 60 min were incubated with PBS-G buffer in the absence of FITC-insulin for a specified period. (A) The intactness of FITC-insulin was evaluated with a fluoroimage analyzer after separation by SDS-PAGE. (B) The vertical axis shows the normal scale. (C) The vertical axis shows a logarithmic scale. Each point represents the mean ± S.E.M. of three monolayers.

Fig. 6. Effects of megalin siRNA transfection on the expression levels of mRNA and protein in RLE-6TN cells. RLE-6TN cells were transfected with control or megalin siRNA for 48 hr. (A) The expression levels of megalin mRNA were measured by real-time PCR analysis. (B) The expression levels of megalin protein were measured by Western blot analysis. Each point represents the mean ± S.E.M. of three monolayers. *$P<0.05$ and **$P<0.01$, significantly different from each control.

Fig. 7. Effects of megalin silencing on the uptake of [^{3}H]gentamicin and FITC-insulin by RLE-6TN cells. RLE-6TN cells were transfected with control or megalin siRNA for 48 hr. The uptake amount of [^{3}H]gentamicin (A) or FITC-insulin (B) for 60 min was measured at 37°C or 4°C after transfection. Specific uptake was estimated by subtracting the cell surface binding at 4°C from the total cell association at 37°C. Each point represents the mean ± S.E.M. of three monolayers. *$P<0.05$, significantly different from each control.

Fig. 8. Expression of insulin receptor (A) and effects of insulin receptor (IR) siRNA transfection on IR mRNA expression (B) and the uptake of FITC-insulin by RLE-6TN cells (C). (A) The expression levels of IR in RLE-6TN cells and primary cultured alveolar type II epithelial cells (AT II) were measured by RT-PCR analysis. (B) IR mRNA was measured after transfection of control or IR siRNA by real-time PCR. (C) Specific uptake of FITC-insulin was estimated in the cells transfected with control siRNA or IR siRNA. Each point represents the mean ± S.E.M. of six monolayers (B, C). *$P<0.05$, significantly different from each control.

Figure

Fig. 1.

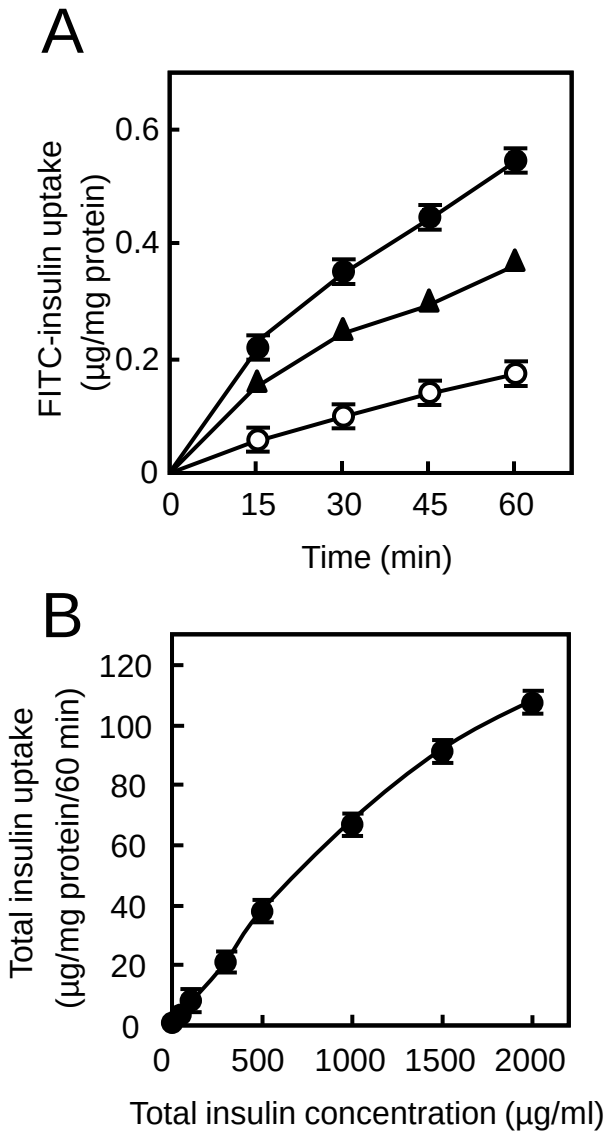
A
FITC-insulin uptake
(μg/mg protein)
0.6
0.4
0.2
0
0
15
30
45
60
Time (min)
B
Total insulin uptake
(μg/mg protein/60 min)
120
100
80
60
40
20
0
0
500
1000
1500
2000
Total insulin concentration (μg/ml)

Fig. 2.

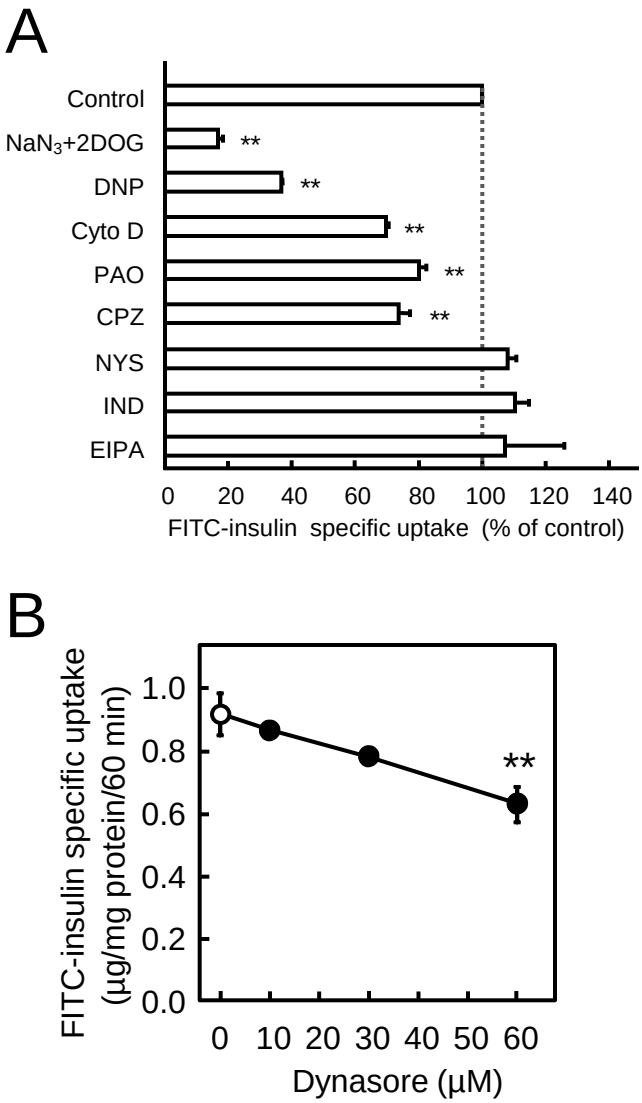
A
Control
NaN3+2DOG
DNP
Cyto D
PAO
CPZ
NYS
IND
EIPA
**
0 20 40 60 80 100 120 140
FITC-insulin specific uptake (% of control)
B
FITC-insulin specific uptake (μg/mg protein/60 min)
1.0
0.8
0.6
0.4
0.2
0.0
**
0 10 20 30 40 50 60
Dynasore (μM)

Fig. 3.

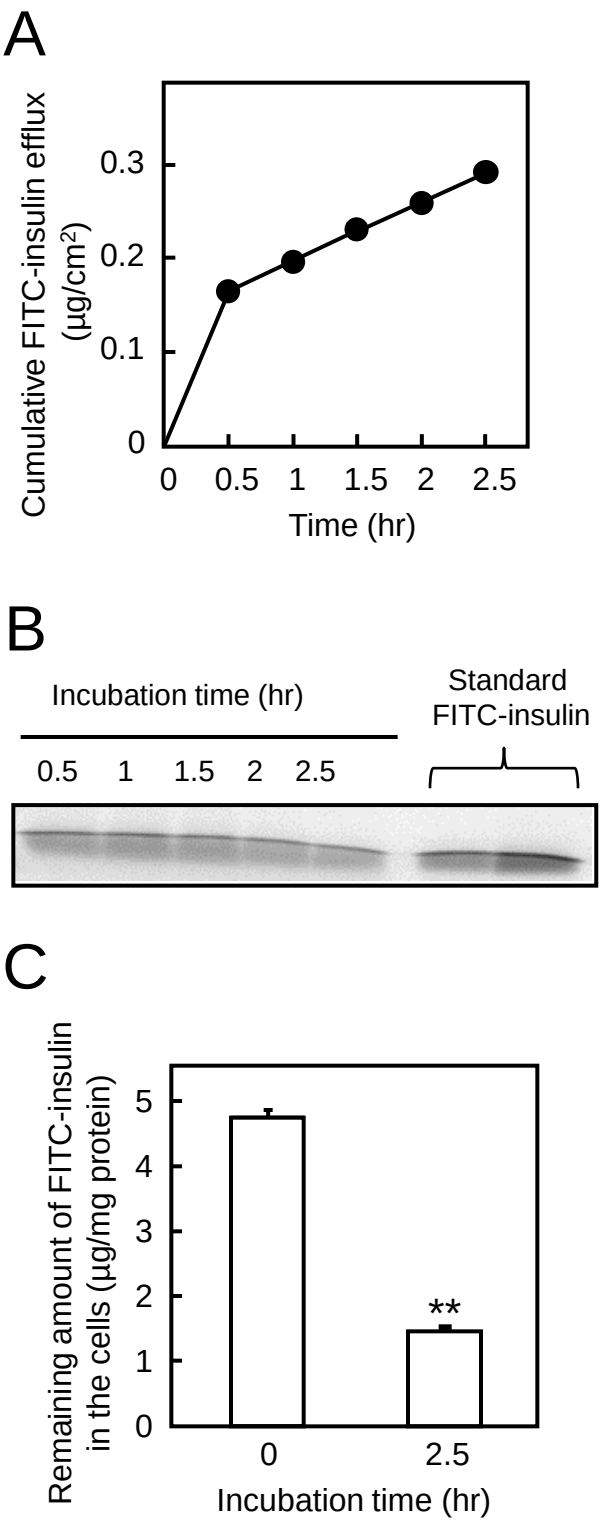
A
Cumulative FITC-insulin efflux (μg/cm²)
0.3
0.2
0.1
0
0 0.5 1 1.5 2 2.5
Time (hr)
B
Incubation time (hr)
Standard FITC-insulin
0.5 1 1.5 2 2.5
C
Remaining amount of FITC-insulin in the cells (μg/mg protein)
5
4
3
2
1
0
**
0 2.5
Incubation time (hr)

Fig. 4.

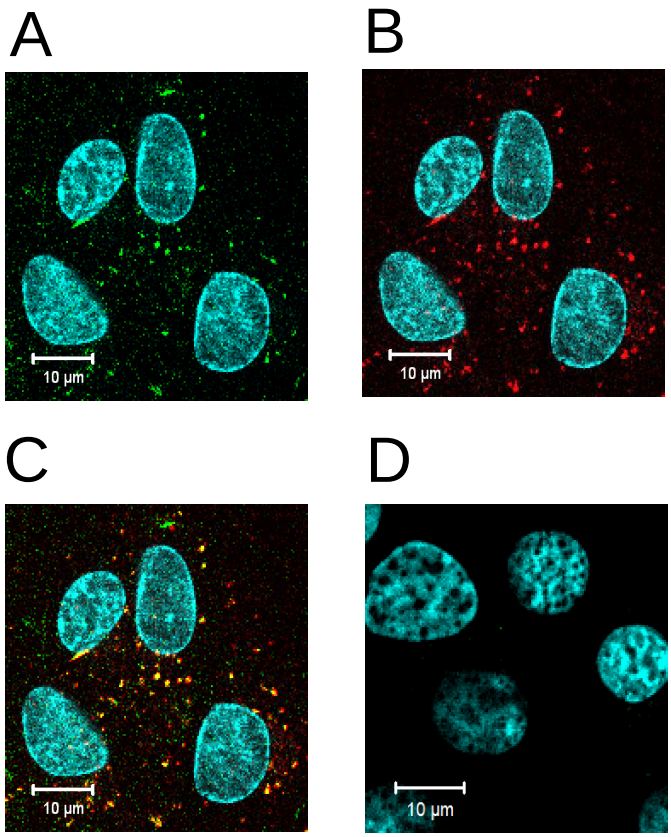

Fig. 5.

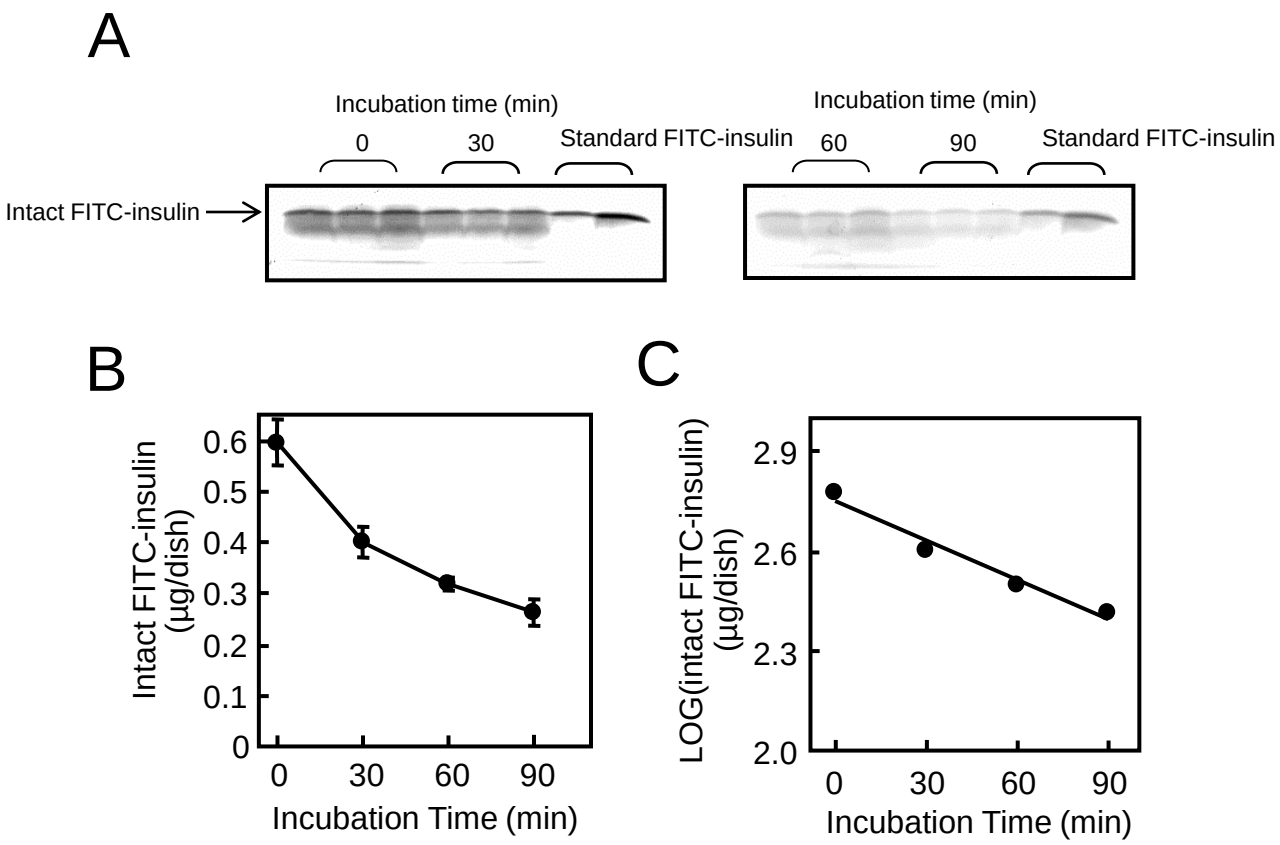
A
Incubation time (min)
0
30
Standard FITC-insulin
Incubation time (min)
60
90
Standard FITC-insulin
Intact FITC-insulin
B
Intact FITC-insulin (µg/dish)
0.6
0.5
0.4
0.3
0.2
0.1
0
0
30
60
90
Incubation Time (min)
C
LOG(intact FITC-insulin) (µg/dish)
2.9
2.6
2.3
2.0
0
30
60
90
Incubation Time (min)

Fig. 6.

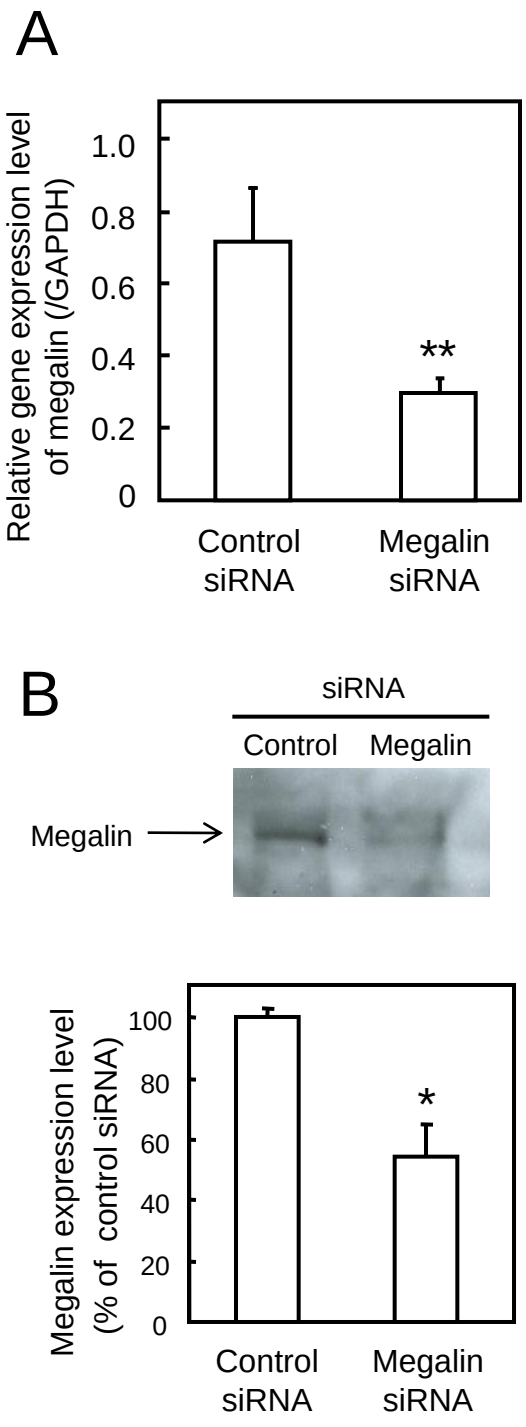
A
Relative gene expression level of megalin (/GAPDH)
1.0
0.8
0.6
0.4
0.2
0
**
Control siRNA
Megalin siRNA
B
siRNA
Control
Megalin
Megalin
Megalin expression level (% of control siRNA)
100
80
60
40
20
0
*
Control siRNA
Megalin siRNA

Fig. 7.

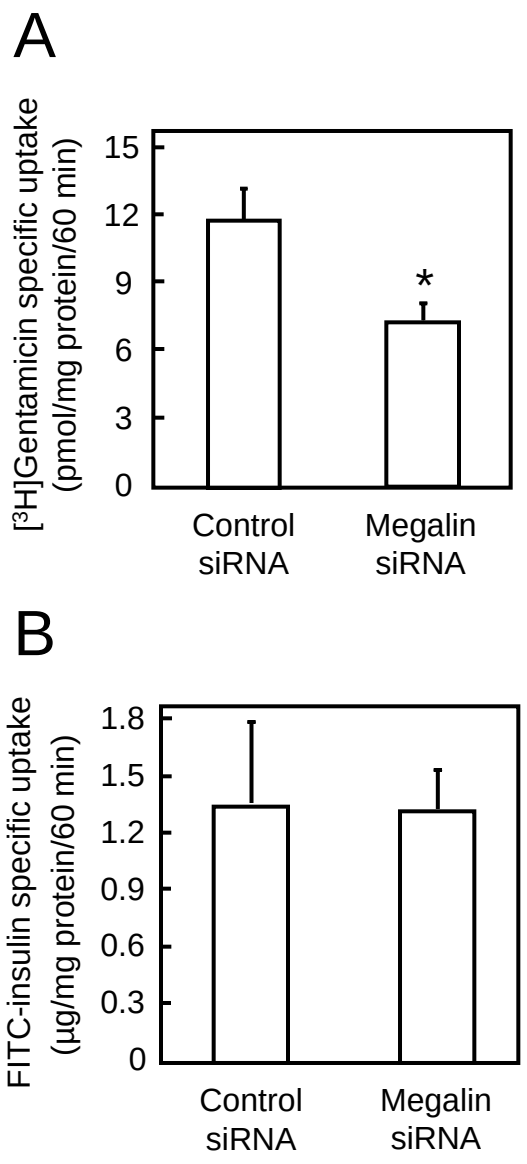
A
[3H]Gentamicin specific uptake
(pmol/mg protein/60 min)
15
12
9
6
3
0
*
Control
siRNA
Megalin
siRNA
B
FITC-insulin specific uptake
(μg/mg protein/60 min)
1.8
1.5
1.2
0.9
0.6
0.3
0
Control
siRNA
Megalin
siRNA

Fig. 8.

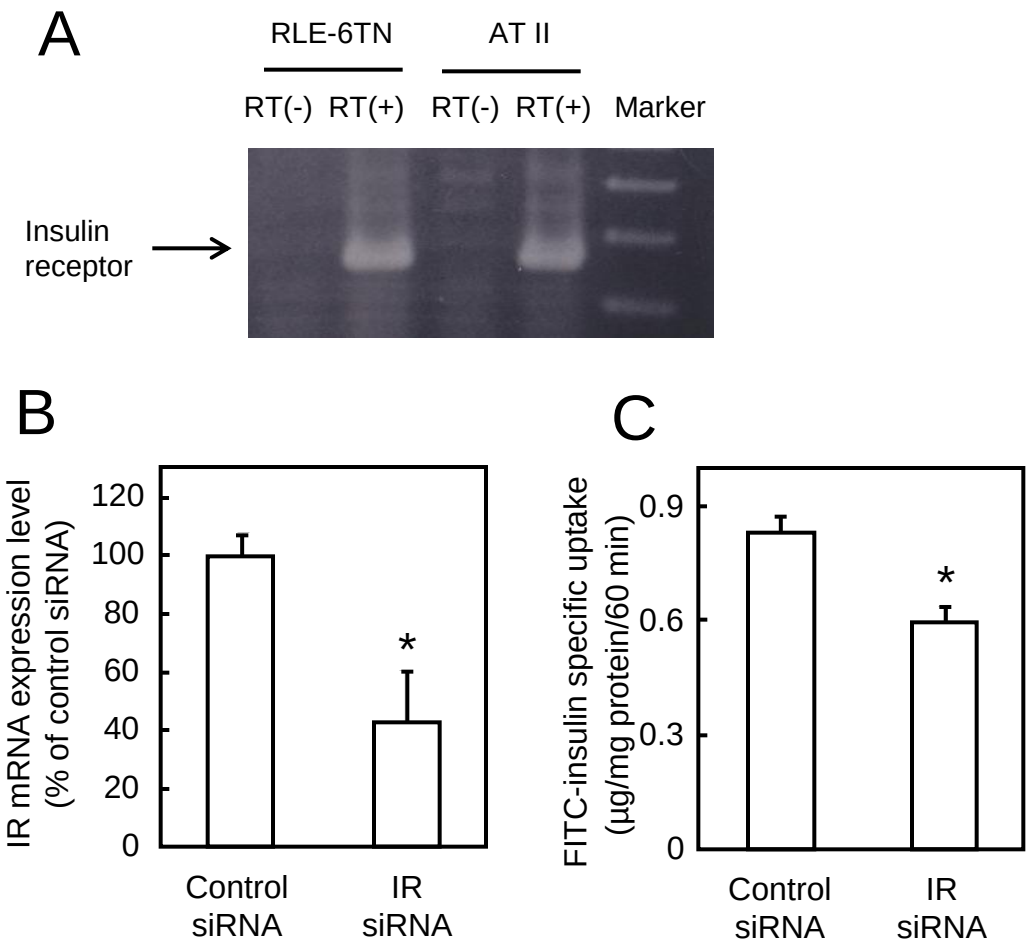
A
RLE-6TN
AT II
RT(-) RT(+) RT(-) RT(+) Marker
Insulin receptor
B
IR mRNA expression level (% of control siRNA)
120
100
80
60
40
20
0
*
Control siRNA
IR siRNA
C
FITC-insulin specific uptake (μg/mg protein/60 min)
0.9
0.6
0.3
0
*
Control siRNA
IR siRNA